

# Heisenberg limit in phase measurements: the threshold detection approach

D. I. Salykina,<sup>1,2</sup> V. S. Liamin,<sup>2,3</sup> V. L. Gorshenin,<sup>2,3</sup> B. N. Nougmanov,<sup>2,3</sup> and F. Ya. Khalili<sup>2,\*</sup>

<sup>1</sup>*Faculty of Physics, M.V.Lomonosov Moscow State University,*

*Leninskie Gory 1, Moscow 119991, Russia*

<sup>2</sup>*Russian Quantum Center, Skolkovo IC, Bolshoy Bulvar 30, bld. 1, Moscow, 121205, Russia*

<sup>3</sup>*Moscow Institute of Physics and Technology, 141700 Dolgoprudny, Russia*

(Dated: 01:53 of 19/12/25)

We analyze the fundamental limits of phase measurement precision, provided by the standard (single- and two-arm) optical interferometers using the Gaussian (squeezed coherent) quantum states of the probing light. We consider two types of the measurements of the output light — the homodyne measurement and the non-linear threshold measurement that provides the sensitivity saturating the quantum Cramer-Rao bound.

For all considered cases, we calculate the best sensitivity  $\Delta\phi_0$  achievable at some given value of phase and the range  $\delta\phi$  around this value within which the sensitivity is close to  $\Delta\phi_0$ . We show that in all cases, the Heisenberg scaling  $\Delta\phi = K/N$  can be reached, where  $K \sim 1$  is a numerical prefactor and  $N$  is the mean photon number. We show also that  $\delta\phi$  strongly depends on  $K$ .

## I. INTRODUCTION

Measurement of the phase of light using optical interferometers is one of the key tasks of experimental physics. The sensitivity of the best modern interferometers is very high and to a major extent is limited by quantum fluctuations of the probing light, see *e.g.* the review papers [1–3]. In particular, if the ordinary coherent state of light is used, then the best possible sensitivity corresponds to the Shot Noise Limit (SNL), equal to

$$\Delta\phi_{\text{SNL}} = \frac{1}{2\sqrt{N}}, \quad (1)$$

where  $\Delta\phi$  is the mean square phase measurement error and  $N$  is the mean photon number interacting with the phase shifting object(s). Better sensitivity, for the same value of  $N$ , can be achieved by using more advanced quantum states. In particular, it was proposed in Ref. [4] to use Gaussian quadrature-squeezed states for this purpose. It was shown in that work that in the case of moderate squeezing,  $e^{2r} \ll N$ , where  $r$  is the logarithmic squeeze factor, the measurement error  $\Delta\phi$  can be suppressed by  $e^r$ , giving the squeezing-enhanced SNL:

$$\Delta\phi_{\text{sqz}} = \frac{e^{-r}}{2\sqrt{N}}. \quad (2)$$

The most sensitive contemporary optical interferometers, namely the laser gravitational-wave detectors, like LIGO [5] or VIRGO [6], use this approach. As a result, they can measure the relative elongations of their multi-kilometer length arms with precision of about  $\sim 10^{-23} \text{ Hz}^{-1/2}$  [7].

\* [farit.khalili@gmail.com](mailto:farit.khalili@gmail.com)

In the ultimate case of very strong squeezing,  $e^{2r} \sim N$ , the sensitivity could reach the so-called Heisenberg limit (HL) [2, 8]:

$$\Delta\phi_{\text{HL}} \sim \frac{K}{N}, \quad (3)$$

where  $K \sim 1$  is a numerical factor. The same result could also be obtained using more exotic non-Gaussian quantum states of light [1, 9–12]. But, unfortunately, the non-Gaussian states are notoriously sensitive to the optical losses and are very hard to prepare [13].

Opposite to the well-established limits (1) and (2), the HL is still a subject of discussion. Various specific forms of the HL (3) and different values of the parameter  $K$  can be found in literature. In addition, in some works the sensitivity is calculated assuming given mean photon number, while in others — assuming given total photon number. Reviews of the various approaches to the HL can be found in Refs. [1, 14, 15].

For example, in Refs. [16–19], the following sensitivity limit was obtained for the given mean photon number  $N$  and an exotic non-Gaussian state:

$$\Delta\phi_{\text{HL}} \approx \frac{1.38}{N}. \quad (4)$$

At the same time, Gaussian squeezed state and the standard homodyne measurement allows to reach the sensitivity noticeably exceeding this value, see Eq (35) below. This discrepancy could be explained by the influence of a priori information on the measurement, see, in particular, Refs. [15, 20, 21]. Note, indeed, that the bound (4) holds for any value of  $\phi$ . At the same time, the limit (35) can be approached only in a narrow range of the values of  $\phi$  with the width  $\sim 1/N$  around some given value of the phase, see Eq. (32).

In this paper, we calculate the sensitivity limits, achievable by the standard optical interferometers using the Gaussian (squeezed coherent) quantum states. We take into account a priori information on the phase by calculating the width  $\delta\phi$  of the range within which the measurement error does not degrade significantly in comparison to the best possible value  $\Delta\phi_0$ , see Eq. (69). Evidently, if the a priori distribution fits into this range, then the resulting measurement error can be approximated by  $\Delta\phi_0$ .

We consider two most important from the practical point of view interferometric topologies, the single-arm and the antisymmetric two-arm ones (see *e.g.* the review [3]). The conceptually more simple single-arm topology, see Fig. 1, directly implements measurement of the phase shift  $\phi$  in a harmonic oscillator mode.

In the two-arm configuration, shown in Fig. 2 (the Mach-Zehnder topology is depicted; it is known, however, that the Michelson one is equivalent to it), the phase shifts are introduced antisymmetrically into the first and the second arms, respectively, and both beamsplitters are the balanced 50%/50% ones. This configuration is insensitive to the common phase shift and therefore more tolerant to technical noises and drifts. Due to this reason, it is used, in particular, in the GW detectors [22, 23].

We consider two types of specific measurement procedures. The first one is the well-known homodyne detector, which is widely used in high-precision experiments. Yet another commonly used detection procedure is the photon number counting, see *e.g.* Refs. [1, 24–26]; we do not consider it here because it gives the results that are close but inferior to the ones of the homodyne detection.

The second procedure which we discuss here is the non-linear threshold detector proposed in Ref. [27] for detection of binary (yes/no) signals. Here we adapt it to the problem of estimation a continuous variable. The key feature of this type of measurement is that for one given value of  $\phi$ ,

it automatically saturates the quantum Cramer-Rao bound (QCRB), which gives the fundamental lower bound for the measurement imprecision [28].

This paper is organized as follows. In the introductory Sec. II, we familiarize the readers with the concepts of QCRB and threshold measurement. In Sections III and IV we analyze the single-arm and two-arm interferometers, respectively. In Sec. V, we summarize the obtained results.

## II. QUANTUM CRAMER-RAO BOUND AND THE THRESHOLD DETECTOR

*a. Quantum Cramer-Rao bound.* Let us start with the QCRB. Let  $\hat{\rho}(\phi)$  be the density operator of an object, depending on the real parameter  $\phi$  (e.g. the phase) that has to be estimated. It can be shown, see Sec. VIII of the monograph Ref. [28], that the lower bound for the variance of an unbiased estimate of  $\phi$  exists, which does not depend on the measurement procedure and has the following form:

$$(\Delta\phi_{\text{QCRB}})^2 = \frac{1}{\text{Tr}[\hat{\rho}(\phi)\hat{\mathcal{L}}^2(\phi)]}, \quad (5)$$

where  $\hat{\mathcal{L}}(\phi)$  is the symmetric logarithmic derivative defined by the following equation:

$$\frac{\partial\hat{\rho}(\phi)}{\partial\phi} = \hat{\rho}(\phi) \circ \hat{\mathcal{L}}(\phi). \quad (6)$$

Here and in the rest of this paper “ $\circ$ ” means symmetrized product, that is, for any operators  $\hat{Q}$  and  $\hat{P}$ ,

$$\hat{Q} \circ \hat{P} = \frac{1}{2}(\hat{Q}\hat{P} + \hat{P}\hat{Q}). \quad (7)$$

We assume in this paper that the quantum state of the probing light is a pure one and has the following form:

$$\hat{\rho}(\phi) = \hat{\mathcal{R}}(\phi)|\psi_0\rangle\langle\psi_0|\hat{\mathcal{R}}^\dagger(\phi), \quad (8)$$

where

$$\hat{\mathcal{R}}(\phi) = e^{-i\hat{N}\phi} \quad (9)$$

it the unitary phase shift operator and  $\hat{N}$  is a Hermitian operator. It was shown in Ref. [28] that in this case Eq. (5) can be presented in the following closed form:

$$(\Delta\phi_{\text{QCRB}})^2 = \frac{1}{4(\Delta\mathcal{N})^2}, \quad (10)$$

where  $(\Delta\mathcal{N})^2$  is the variance of  $\hat{N}$  in the state (8).

*b. Threshold detector.* It is known that the measurement of  $\hat{\mathcal{L}}$  saturates the QCRB, see Ref. [28]. Its application to the phase measurement with Gaussian states of light was considered in Ref. [29]. Semi-gedanken implementation of this measurement, based on the second order optical nonlinearity, was proposed in Ref. [30].

Note however that the operator  $\hat{\mathcal{L}}$  explicitly depends on  $\phi$  (while the QCRB itself does not). This feature creates a “vicious loop”: in order to measure  $\phi$ , we have to know its value in advance. Therefore, let us consider an adapted to the measurement of a continuous variable version of threshold detection, initially proposed in [27] (see also Sec. IV.3 of [28]). Suppose that some Hermitian operator  $\hat{Y}$  is measured, and we are interested in the sensitivity at some given value of  $\phi = \phi_0$ . Without limiting the generality, we assume that  $\phi_0 = 0$ . Using the error propagation

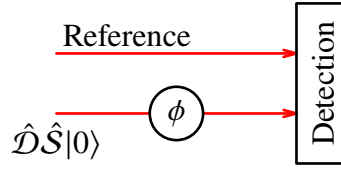


FIG. 1. The single-arm interferometer.

approach, the estimation error  $\Delta\phi_0$ , corresponding to the vanishingly small values of  $\phi \rightarrow 0$  (the threshold sensitivity) can be calculated as follows:

$$(\Delta\phi_0)^2 = \frac{(\Delta Y)^2}{G^2} \Big|_{\phi \rightarrow 0}, \quad (11)$$

where

$$(\Delta Y)^2 = \text{Tr}[\hat{\rho}(\phi)\hat{Y}^2] - (\text{Tr}[\hat{\rho}(\phi)\hat{Y}])^2 \quad (12)$$

is the variance of  $\hat{Y}$  and

$$G = \frac{\partial \text{Tr}[\hat{\rho}(\phi)\hat{Y}]}{\partial \phi} \quad (13)$$

is the gain factor.

It can be shown that the minimum of the uncertainty (11) is provided by the operator  $\hat{Y}$ , which satisfies the following equation:

$$\lim_{\phi \rightarrow 0} \frac{\partial \hat{\rho}(\phi)}{\partial \phi} = \hat{\rho}(0) \circ \hat{Y}. \quad (14)$$

It follows from Eqs. (13) and (14) that

$$\text{Tr}[\hat{\rho}(0)\hat{Y}] = 0, \quad G|_{\phi=0} = (\Delta Y)^2|_{\phi=0} \quad (15)$$

and therefore,

$$(\Delta\phi_0)^2 = \frac{1}{(\Delta Y)^2} \Big|_{\phi \rightarrow 0}. \quad (16)$$

It is easy to note that up to the notations, in the case of  $\phi \rightarrow 0$ , Eq. (6) is identical to Eq. (14). Therefore, the measurement of  $\hat{Y}$  saturates the QCRB in this particular case, compare Eqs. (5) and (16).

It is natural to expect that for smooth  $\hat{\rho}(\phi)$  and for sufficiently small values of  $\phi$ , this measurement should provide a good sensitivity, approaching the QCRB, albeit may be not reaching it exactly. The corresponding measurement error in this case can be calculated using the generic error propagation formula

$$(\Delta\phi)^2 = \frac{(\Delta Y)^2}{G^2}. \quad (17)$$

This approach will be used in the next sections.

### III. SINGLE-ARM INTERFEROMETER

*a. The scheme.* Let us consider the single-arm interferometer shown in Fig. 1. We suppose that the input beam is prepared in the Gaussian squeezed coherent state

$$|\psi_0\rangle = \hat{\mathcal{D}}\hat{\mathcal{S}}|0\rangle. \quad (18)$$

Here  $|0\rangle$  is the ground state,

$$\hat{\mathcal{D}} = e^{\alpha(\hat{a}^\dagger - \hat{a})} \quad (19)$$

is the displacement operator, where we assume without limiting the generality that the displacement parameter  $\alpha$  is real,  $\hat{a}$ ,  $\hat{a}^\dagger$  are, respectively, the annihilation and creation operators, and

$$\hat{\mathcal{S}} = e^{r(\hat{a}^\dagger 2 - \hat{a}^2)/2} \quad (20)$$

is the squeeze operator with the real and non-negative squeeze factor  $r$ . This choice of  $r$  corresponds to the squeezed phase quadrature of the input light and therefore to the best phase sensitivity for a given  $r$ , see Refs. [3, 4]. It is easy to show that the mean value  $N$  and the variance  $(\Delta N)^2$  of the number of quanta

$$\hat{N} = \hat{a}^\dagger \hat{a} \quad (21)$$

in the state (18) are equal to

$$N = \alpha^2 + \sinh^2 r, \quad (22)$$

$$(\Delta N)^2 = \alpha^2 e^{2r} + \frac{1}{2} \sinh^2 2r. \quad (23)$$

Using the Heisenberg picture, evolution of optical fields in scheme can be described by the following input/output relations (see *e.g.* Ref. [3]):

$$\begin{pmatrix} \hat{x}_{\text{out}} \\ \hat{p}_{\text{out}} \end{pmatrix} = \hat{\mathcal{U}}^\dagger(\phi) \begin{pmatrix} \hat{x} \\ \hat{p} \end{pmatrix} \hat{\mathcal{U}}(\phi) = \begin{pmatrix} (\sqrt{2}\alpha + \hat{x}e^r) \cos \phi + \hat{p}e^{-r} \sin \phi \\ -(\sqrt{2}\alpha + \hat{x}e^r) \sin \phi + \hat{p}e^{-r} \cos \phi \end{pmatrix}, \quad (24)$$

where

$$\hat{\mathcal{U}}(\phi) = \hat{\mathcal{R}}(\phi) \hat{\mathcal{D}} \hat{\mathcal{S}} \quad (25)$$

is the evolution operator,

$$\hat{\mathcal{R}}(\phi) = e^{-i\hat{N}\phi} \quad (26)$$

is the phase shift operator,  $\hat{x}$ ,  $\hat{p}$  are, respectively, the Hermitian amplitude and phase quadrature operators of the input field, defined by

$$\hat{a} = \frac{\hat{x} + i\hat{p}}{\sqrt{2}}, \quad (27)$$

and  $\hat{x}_{\text{out}}$ ,  $\hat{p}_{\text{out}}$  are the corresponding operators of the output field. Note that the squeeze and displacement operations are taken into account in Eqs. (24). Therefore, the operators  $\hat{x}$  and  $\hat{p}$  correspond to the initial vacuum fields and their variances are equal to  $1/2$ .

*b. Homodyne detection.* In the case of the small phase shift,  $|\phi| \ll 1$ , the phase quadrature of the output beam  $\hat{p}_{\text{out}}$  carries the major part of the phase information. Therefore, we consider the homodyne measurement of this quadrature. Using the error propagation method, we obtain that the corresponding measurement error is equal to

$$(\Delta\phi)^2 = \frac{(\Delta p_{\text{out}})^2}{G^2}, \quad (28)$$

where

$$(\Delta p_{\text{out}})^2 = \frac{1}{2}(e^{-2r} \cos^2 \phi + e^{2r} \sin^2 \phi) \quad (29)$$

is the variance of  $\hat{p}_{\text{out}}$  and

$$G = \frac{\partial \langle \hat{p}_{\text{out}} \rangle}{\partial \phi} = -\sqrt{2}\alpha \cos \phi \quad (30)$$

is the gain factor.

If  $r \neq 0$ , then the variance (29) depends on  $\phi$ , and if  $r > 0$ , then it increases with the increase of  $\phi$ , limiting the high sensitivity range  $\delta\phi$ . Note also that the two terms in parentheses in Eq. (29) are related by the uncertainty principle. Therefore, the stronger the squeezing and therefore the better the sensitivity at  $\phi = 0$ , the bigger the second term. As a result,  $\delta\phi$  scales with  $r$  as  $e^{-2r}$ .

In order to present Eq. (28) in HL-like form, we minimize it in  $\alpha^2$  under the condition (22). To find the best possible sensitivity, we perform this optimization at  $\phi = 0$ . In this case, the minimum is achieved at

$$\alpha^2 = \frac{N(N+1)}{2N+1}. \quad (31)$$

In this case, about half of the optical power is provided by the coherent amplitude and the other part — by the squeezing, see Eq. (22). It is interesting that the same result was obtained in Ref. [24] for the photon number counting case.

Substitution of this value into Eq. (28) gives:

$$(\Delta\phi)^2 = \frac{1 + (2N+1)^2 \tan^2 \phi}{4N(N+1)}. \quad (32)$$

*c. QCRB and threshold detector at  $\phi \rightarrow 0$*  It follows from Eqs. (10), (9), and (26) that the QCRB in the single-arm interferometer case is equal to

$$(\Delta\phi)^2 = \frac{1}{4(\Delta N)^2}, \quad (33)$$

where the photon number variance is given by Eq. (23). Minimizing it in  $\alpha^2$  under the condition (22) and taking into account that  $\alpha^2 \geq 0$ , we obtain that the minimum is provided by

$$\alpha = 0, \quad (34)$$

and is equal to

$$(\Delta\phi_0)^2 = \frac{1}{8N(N+1)}. \quad (35)$$

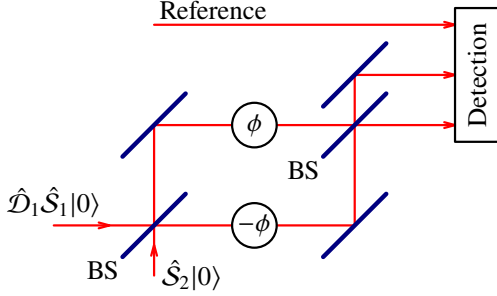


FIG. 2. The antisymmetric two-arm interferometer. BS: 50%/50% beam splitters.

*d. Threshold detector at  $\phi \neq 0$ .* In order to calculate the measurement error for other values of  $\phi$ , the explicit form of the operator  $\hat{Y}$  is required. It is shown in App. A that it can be presented in the following bilinear form, compare with Refs. [29, 31, 32]:

$$\hat{Y} = -2\hat{p} \circ (\sqrt{2}\alpha \cosh 2r + \hat{x} \sinh 2r). \quad (36)$$

In the Heisenberg picture, the value of this operator at the output of the interferometer is equal to

$$\hat{Y}_{\text{out}} = \hat{\mathcal{U}}^\dagger(\phi) \hat{Y} \hat{\mathcal{U}}(\phi) = -2\hat{p}_{\text{out}} \circ (\sqrt{2}\alpha \cosh 2r + \hat{x}_{\text{out}} \sinh 2r), \quad (37)$$

see Eqs. (24).

Now we are in a position to calculate the phase measurement error for all values of  $\phi$ , using the error propagation method. We assume the same value of  $\alpha = 0$  that gives the best possible sensitivity at  $\phi = 0$ , see Eq. (34). In this case, it follows from Eqs. (22), (24), and (37) that the mean value and the variance of  $\hat{Y}_{\text{out}}$  are equal to

$$\langle \hat{Y}_{\text{out}} \rangle = 4N(N+1) \sin 2\phi, \quad (38a)$$

$$(\Delta Y_{\text{out}})^2 = 8[1 + 4N(N+1) \sin^2 2\phi]N(N+1). \quad (38b)$$

Therefore,

$$(\Delta\phi)^2 = \frac{(\Delta Y_{\text{out}})^2}{G^2} = \frac{1 + 4N(N+1) \sin^2 2\phi}{8N(N+1) \cos^2 2\phi}, \quad (39)$$

where

$$G = \frac{\partial \langle \hat{Y}_{\text{out}} \rangle}{\partial \phi} = 8N(N+1) \cos 2\phi. \quad (40)$$

#### IV. TWO-ARM INTERFEROMETER

*a. The scheme.* The antisymmetric two-arm interferometer which we consider here is shown in Fig. 2. We assume that both beam splitters are described by the following reflectivity/transmissivity matrix:

$$\mathbb{B} = \frac{1}{\sqrt{2}} \begin{pmatrix} 1 & 1 \\ 1 & -1 \end{pmatrix}, \quad (41)$$

and in the absence of the phase shifts  $\pm\phi$ , the arm lengths are equal to each other. In this case, at  $\phi = 0$  both input states are reproduced at the respective bright and dark output ports (the dark fringe regime).

Note that in literature, the signal phase shifts are often denoted as  $\pm\phi/2$ . Here we use the “ $\pm\phi$ ” convention, because it is more consistent with the single arm case, providing the same values of the SNL (1) and the squeezing-enhanced SNL (2) as the single-arm interferometer.

Following Refs. [4, 33], we assume that the squeezed coherent state is injected into the first (bright) input port, and the squeezed vacuum state — into the second (dark) input port. This combination gives the equal values of the mean optical power in two arms, keeping the (anti-) symmetry of the scheme intact, see Refs. [3, 34].

The corresponding two-mode input wave function is the following:

$$|\psi_{0,0}\rangle = \hat{\mathcal{D}}_1 \hat{\mathcal{S}}_1 \hat{\mathcal{S}}_2 |0,0\rangle. \quad (42)$$

Here  $|0,0\rangle$  is the two-mode ground state,

$$\hat{\mathcal{D}}_1 = e^{\alpha(\hat{a}_1^\dagger - \hat{a}_1)} \quad (43)$$

is the displacement operator of the first (bright) input mode,

$$\hat{\mathcal{S}}_1 = e^{R(\hat{a}_1^\dagger)^2 - \hat{a}_1^2}/2, \quad \hat{\mathcal{S}}_2 = e^{r(\hat{a}_2^\dagger)^2 - \hat{a}_2^2}/2 \quad (44)$$

are, respectively, the squeeze operators of the first and second modes, and  $\hat{a}_{1,2}$  and  $\hat{a}_{1,2}^\dagger$  are the corresponding creation and annihilation operators of the input field (before the first beamsplitter). Similarly to the single-arm case, we assume that the parameters  $\alpha$ ,  $R$  and  $r$  are real (see also Ref. [3]). It is easy to show that in this case, the mean value of the sum photon number in the interferometer is equal to

$$N = \alpha^2 + \sinh^2 R + \sinh^2 r. \quad (45)$$

The phase shift operator (9) in the antisymmetric two-arm case has the following form:

$$\hat{\mathcal{R}}_-(\phi) = e^{-i\hat{N}_-\phi}, \quad (46)$$

where

$$\hat{N}_- = \hat{b}_1^\dagger \hat{b}_1 - \hat{b}_2^\dagger \hat{b}_2 = \hat{a}_1^\dagger \hat{a}_2 + \hat{a}_2^\dagger \hat{a}_1, \quad (47)$$

is the difference of the photon numbers in the arms and

$$\hat{b}_1 = \frac{\hat{a}_1 + \hat{a}_2}{\sqrt{2}}, \quad \hat{b}_2 = \frac{\hat{a}_1 - \hat{a}_2}{\sqrt{2}}. \quad (48)$$

are the annihilation operators for the intracavity fields before the phase shifts, see Eq. (41). It follows from Eqs. (42) and (47) that the variance of  $\hat{N}_-$  is equal to

$$(\Delta N_-)^2 = \alpha^2 e^{2r} + \sinh^2(R + r). \quad (49)$$

In the Heisenberg evolution picture, the input/output relations for the two-arm interferometer are the following, see Ref. [3]:

$$\begin{pmatrix} \hat{x}_{1 \text{ out}} \\ \hat{p}_{1 \text{ out}} \\ \hat{x}_{2 \text{ out}} \\ \hat{p}_{2 \text{ out}} \end{pmatrix} = \hat{\mathcal{U}}_-^\dagger(\phi) \begin{pmatrix} \hat{x}_1 \\ \hat{p}_1 \\ \hat{x}_2 \\ \hat{p}_2 \end{pmatrix} \hat{\mathcal{U}}_-(\phi) = \begin{pmatrix} (\sqrt{2}\alpha + \hat{x}_1 e^R) \cos \phi + \hat{p}_2 e^{-r} \sin \phi \\ -\hat{x}_2 e^r \sin \phi + \hat{p}_1 e^{-R} \cos \phi \\ \hat{x}_2 e^r \cos \phi + \hat{p}_1 e^{-R} \sin \phi \\ -(\sqrt{2}\alpha + \hat{x}_1 e^R) \sin \phi + \hat{p}_2 e^{-r} \cos \phi \end{pmatrix}, \quad (50)$$

where

$$\hat{\mathcal{U}}_-(\phi) = \hat{\mathcal{R}}_-(\phi) \hat{\mathcal{D}}_1 \hat{\mathcal{S}}_1 \hat{\mathcal{S}}_2 \quad (51)$$

is the two-mode evolution operator,  $\hat{x}_{1,2}$ ,  $\hat{p}_{1,2}$  are the amplitude and phase quadrature operators of the input fields, defined by

$$\hat{a}_{1,2} = \frac{\hat{x}_{1,2} + i\hat{p}_{1,2}}{\sqrt{2}}, \quad (52)$$

and  $\hat{x}_{1,2 \text{ out}}$ ,  $\hat{p}_{1,2 \text{ out}}$  are the corresponding operators of the output fields.

*b. Homodyne detector.* Similarly to the single-arm scheme [compare Eqs. (24) and (50)], we consider the homodyne measurement of the quadrature  $\hat{p}_{2 \text{ out}}$  which carries the major part of the phase information, see Eq. (50). In this case,

$$(\Delta\phi)^2 = \frac{(\Delta p_{2 \text{ out}})^2}{G^2}, \quad (53)$$

where

$$(\Delta p_{2 \text{ out}})^2 = \frac{1}{2}(e^{-2r} \cos^2 \phi + e^{2R} \sin^2 \phi) \quad (54)$$

is the variance of the measured quadrature and  $G = \partial \langle \hat{p}_{2 \text{ out}} \rangle / \partial \phi$  is the gain factor that again is equal to (30).

Note that now, opposite to the single-arm case, two components of  $\Delta p_{2 \text{ out}}$  originate from two independent input modes and does not bound by the uncertainty relation. Therefore, increase of the squeeze factor  $r$  does not affect the second term in Eq. (54), proportional to  $e^{2R}$ . As a result, much broader range  $\delta\phi$  could be achieved in the two-arm case.

Let us minimize Eq. (53) in  $\alpha^2$  under the condition (45) at the best sensitivity point of  $\phi = 0$ . In order to avoid over-cluttering of the equations, we consider in more detail two most interesting particular cases: the canonical single-squeezed case of  $R = 0$  and the anti-symmetrically double-squeezed one of  $R = -r$ . The evident third option is the symmetrically double-squeezed one,  $R = r$ . However, calculations show that it provides the results similar to the considered in Sec. III single-arm case, but slightly inferior to it. Therefore, we do not consider it here.

In the first case,

$$(\Delta p_{2 \text{ out}})^2 = \frac{1}{2}(e^{-2r} \cos^2 \phi + \sin^2 \phi), \quad (55)$$

the optimum is provided by

$$\alpha^2 = \frac{N(N+1)}{2N+1} \quad (56)$$

and is equal to

$$(\Delta\phi)^2 = \frac{1 + (2N+1) \tan^2 \phi}{4N(N+1)}. \quad (57)$$

see also Ref. [35].

In the second case,  $\Delta p_{2 \text{ out}}$  does not depend on  $\phi$ :

$$(\Delta p_{2 \text{ out}})^2 = \frac{e^{-2r}}{2}, \quad (58)$$

Correspondingly,

$$\alpha^2 = \frac{N(N+2)}{2(N+1)}, \quad (59)$$

and

$$(\Delta\phi)^2 = \frac{1}{2N(N+2) \cos^2 \phi}. \quad (60)$$

c. *QCRB and threshold detector at  $\phi \rightarrow 0$ .* It follows from Eqs. (9) and (46) that the QCRB in the double-arm interferometer case is equal to

$$(\Delta\phi)^2 = \frac{1}{4(\Delta N_-)^2}, \quad (61)$$

where the photon number variance is given by Eq. (49).

We minimize this value under the condition (45) for the same two particular cases that were considered for the homodyne measurement, namely  $R = 0$  and  $R = -r$ . If  $R = 0$ , then the minimum is provided by

$$\alpha^2 \approx \frac{N + 1/4}{2} \quad (62)$$

and is equal to

$$(\Delta\phi_0)^2 \approx \frac{1}{4N(N + 3/2)}. \quad (63)$$

In the second case, correspondingly,

$$\alpha^2 = \frac{N(N + 2)}{2(N + 1)} \quad (64)$$

and

$$(\Delta\phi_0)^2 = \frac{1}{2N(N + 2)}. \quad (65)$$

d. *Threshold detector at  $\phi \neq 0$ .* In order to calculate the measurement error for  $\phi \neq 0$ , we again need the explicit form of the operator  $\hat{Y}$ . It is shown in App. B that it has the following, again bilinear, form:

$$\hat{Y} = -2[\sqrt{2}\alpha\hat{p}_2e^{r-R}\cosh(R + r) + (\hat{x}_1\hat{p}_2e^{r-R} + \hat{x}_2\hat{p}_1e^{R-r})\sinh(R + r)]. \quad (66)$$

In the Heisenberg picture, the value of this operator at the output of the interferometer is equal to

$$\hat{Y}_{\text{out}} = 2[\sqrt{2}\alpha\hat{p}_{2\text{out}}e^{r-R}\cosh(R + r) + (\hat{x}_{1\text{out}}\hat{p}_{2\text{out}}e^{r-R} + \hat{x}_{2\text{out}}\hat{p}_{1\text{out}}e^{R-r})\sinh(R + r)]. \quad (67)$$

Consider again the same two particular cases of  $R = 0$  and  $R = -r$ . In the first one, in order to simplify the equations, we assume that  $|\phi| \ll 1$ . The corresponding values of the gain factor  $G$  and the variance of  $Y_{\text{out}}$  are calculated in App. B, see Eqs. (B14). Substituting the optimization condition (62) into these equations, we obtain that

$$(\Delta\phi)^2 \approx \frac{1 + \frac{1}{2}(9N + 5/4)\phi^2}{4N(N + 3/2)}. \quad (68)$$

In the second particular case of  $R = -r$ , the nonlinear term in Eq. (67) vanishes and  $Y_{\text{out}}$  becomes proportional to the quadrature  $p_{2\text{out}}$ . This means that the homodyne measurement of this quadrature is now the optimal procedure, described by the phase measurement error (60).

	HD		TD	
	$(\Delta\phi_0)^2$	$(\delta\phi)^2$	$(\Delta\phi_0)^2$	$(\delta\phi)^2$
Single-arm	$\frac{1}{4N(N+1)}$	$\frac{1}{N(N+1)}$	$\frac{1}{8N(N+1)}$	$\frac{1}{4N(N+1)}$
Two-arm, $R = 0$	$\frac{1}{4N(N+1)}$	$\frac{2}{N+1/2}$	$\approx \frac{1}{4N(N+3/2)}$	$\approx \frac{8}{9N+5/4}$
Two-arm, $R = -r$	$\frac{1}{2N(N+2)}$	$\sim 1$	$\frac{1}{2N(N+2)}$	$\sim 1$

TABLE I. Optimized sensitivity for the three considered interferometric configurations and for the homodyne detection (HD) and threshold detection (TD) measurement schemes;  $m$ : the configuration number.

## V. DISCUSSION

In the most important from the practical point of view case of the big mean photon number  $N \gg 1$  and the small signal phase shift  $|\phi| \ll 1$ , the sensitivity limits (32), (39), (57), (60), and (68), calculated in Sections III and IV, can be presented in the following unified form:

$$(\Delta\phi)^2 \Big|_{\phi} \approx (\Delta\phi_0)^2 \times \left(1 + \frac{4\phi^2}{(\delta\phi)^2}\right). \quad (69)$$

The values of  $\Delta\phi_0$  and  $\delta\phi$  for the configurations considered in this paper are presented in Table I. It can be seen that in all cases, the HL scaling (3) can be achieved, but with different values of the factor  $K$ . It can be seen also that there is an interdependence between values the values of  $\Delta\phi_0$  and  $\delta\phi$ . In all cases except for the single-arm interferometer with the homodyne detection, it can be roughly estimated as follows:

$$\log_N(\delta\phi) \sim \log_2(N\Delta\phi_0) + \frac{1}{2}. \quad (70)$$

In almost all considered cases, the ordinary homodyne detector provides virtually the same sensitivity, both in terms of  $\Delta\phi_0$  and  $\delta\phi$ , as the non-linear threshold detector. The only exception is the single arm interferometer, where threshold detector gives twice as small value of  $(\Delta\phi_0)^2$ , which corresponds to the best sensitivity among all considered here cases. At the same time, the single-arm interferometer is characterized by the most narrow range of high sensitivity,  $\delta\phi \sim 1/N$  for both the homodyne and threshold detection cases. Note that it is close to  $\Delta\phi_0$ , that is, in this case the a priori knowledge about the phase distribution before the measurement should be as good as measurement precision.

These two features stem from the same origin, namely the enhanced by the squeezing amplitude quadrature of the input light  $\hat{x}e^r$ , which appears in the measured phase quadrature of the output light  $\hat{p}_{\text{out}}$  at  $\phi \neq 0$ , see Eq. (24). Note also that this term is bound by the uncertainty relation with the term  $\hat{p}e^{-r}$  which defines the measurement error at  $\phi = 0$ . As a result, the variance  $\Delta p_{\text{out}}$  sharply increases with the increase of  $\phi$ , limiting the value of  $\delta\phi$ .

At the same time, the dependence of  $\Delta p_{\text{out}}$  on  $\phi$  can be exploited as the additional source of information using more advanced data processing or more sophisticated measurements. In particular, in Ref. [24] the use of the maximum likelihood method was considered. The disadvantage of this approach is that it requires multiple measurements, which leads to the additional factor  $\sqrt{p}$  in

the numerator of the HL (3), where  $p$  is the repetitions number. Another approach is the use of a non-linear measurement, in particular, of the threshold detector. It is interesting that in this case the optimization procedure prefers the variance information to the linear one, setting the value of  $\alpha$  equal to zero, see Eq. (34).

In the two-arm interferometer case, the measured output quadrature  $\hat{p}_{\text{out}}$  depends on the quadratures  $\hat{x}_1$  and  $\hat{p}_2$  of the two independently prepared input modes and does not bound by the uncertainty relation. As a result, the squeezing of  $\hat{p}_2$  does not affect uncertainty of  $\hat{x}_1$ , and vice versa. In particular, if the first mode is not squeezed,  $R = 0$ , then the value of  $\delta\phi$  scales only as  $1/\sqrt{N}$ . This feature allows to use, before the main measurement, a preliminary “ranging” shot noise limited one (without squeezing in both arms), which is characterized by  $\delta\phi \sim 1$ , thus providing, in the series of two measurement, both broad  $\delta\phi$  and the HL sensitivity.

Finally, in the double-squeezed case of  $R = -r$ , the variance of  $\hat{p}_{2\text{out}}$  does not depend on  $\phi$  at all, see Eq. (58). As a result, the non-linear term in  $\hat{Y}_{\text{out}}$  vanishes and the threshold detection scheme reduces to the ordinary homodyne measurement. The high sensitivity range in this case is the broadest one,  $\delta\phi \sim 1$ . At the same time, the value of  $(\Delta\phi_0)^2$  is twice as big as in the previous case. This feature can be attributed to the additional term  $\sinh^2 R = \sinh^2 r$  in the expression (45) for the mean number of quanta that leads to the smaller value of  $\alpha$  for the same values of  $N$  and  $r$ . However, it is worth noting that the corresponding HL prefactor  $1/2$  is still smaller than  $\approx 1.38^2$  of the limit (4), despite the exotic non-Gaussian nature of the quantum states providing that limit.

## ACKNOWLEDGMENTS

This work of D.S., V.G., B.N., and F.K. was supported by the Theoretical Physics and Mathematics Advancement Foundation “BASIS” Grant #23-1-1-39-1. Authors thank L. Pezze for his valuable remarks on this work.

## Appendix A: Threshold detection, single-arm interferometer

*a. Threshold detector at  $\phi = 0$ .* In the Schrödinger picture, the output field of the interferometer is described by the following density operator:

$$\hat{\rho}(\phi) = \mathcal{R}(\phi)\hat{\rho}_0\mathcal{R}^\dagger(\phi), \quad (\text{A1})$$

where

$$\hat{\rho}_0 = |\psi_0\rangle\langle\psi_0|. \quad (\text{A2})$$

By substituting it into Eq. (14), we obtain:

$$i[\hat{\rho}_0, \hat{N}] = \hat{\rho}_0 \circ \hat{Y}. \quad (\text{A3})$$

Consider then a set of quantum states  $\{|\psi_k\rangle\}$ , with  $k = 1, 2, \dots$ , complementing  $|\psi_0\rangle$  to the full orthonormal set:

$$\langle\psi_k|\psi_l\rangle = \delta_{kl}, \quad \sum_{k=0}^{\infty} |\psi_k\rangle\langle\psi_k| = \hat{I}, \quad k = 0, 1, \dots \quad (\text{A4})$$

In this representation, Eq. (A3) can be rewritten as follows:

$$i(\delta_{k0}\langle\psi_0|\hat{N}|\psi_l\rangle - \delta_{l0}\langle\psi_k|\hat{N}|\psi_0\rangle) = \frac{1}{2}(\delta_{k0}\langle\psi_0|\hat{Y}|\psi_l\rangle + \delta_{l0}\langle\psi_k|\hat{Y}|\psi_0\rangle). \quad (\text{A5})$$

This equation can be solved explicitly, giving:

$$\langle \psi_k | \hat{Y} | \psi_l \rangle = \begin{cases} 0, & k = l = 0, \\ 2i \langle \psi_0 | \hat{N} | \psi_l \rangle, & k = 0, l > 0, \\ -2i \langle \psi_k | \hat{N} | \psi_0 \rangle, & k > 0, l = 0, \\ \text{undefined}, & k > 0, l > 0. \end{cases} \quad (\text{A6})$$

It is easy to see from this equation, that

$$(\Delta Y)^2 = 4(\Delta N)^2 \quad (\text{A7})$$

With an account for Eq. (16), we obtain Eq. (33).

b. *Threshold detector at  $\phi \neq 0$ .* In order to calculate the measurement error for other values of  $\phi$ , the explicit form of the operator  $\hat{Y}$  is required, that is, the set  $\{|\psi_k\rangle\}$  and the fourth clause in Eq. (A6) have to be defined explicitly. In this paper, following Refs. [29, 31, 32], we consider a simple bilinear in  $\hat{x}$ ,  $\hat{p}$  form of  $\hat{Y}$  that, in principle, could be implemented in an experiment, see Ref. [30].

As the natural orthonormal extension of the state (18), we consider the set of squeezed and displaced Fock states:

$$|\psi_n\rangle = \hat{\mathcal{D}}\hat{\mathcal{S}}|n\rangle, \quad n = 0, 1, \dots, \quad (\text{A8})$$

where the operators  $\hat{\mathcal{D}}$  and  $\hat{\mathcal{S}}$  are given by Eqs. (19) and (20), respectively. In this case, we obtain that if  $l > 0$ , then

$$2i \langle \psi_0 | \hat{N} | \psi_l \rangle = 2i \langle 0 | \hat{\mathcal{S}}^\dagger \hat{\mathcal{D}}^\dagger \hat{a}^\dagger \hat{a} \hat{\mathcal{D}} \hat{\mathcal{S}} | l \rangle = \langle 0 | \hat{Y} | l \rangle, \quad (\text{A9})$$

where

$$\hat{Y} = i(2\alpha \hat{a} e^r + \hat{a}^2 \sinh 2r). \quad (\text{A10})$$

As a result, Eq. (A6) takes the following form:

$$\langle k | \hat{\mathcal{S}}^\dagger \hat{\mathcal{D}}^\dagger \hat{Y} \hat{\mathcal{D}} \hat{\mathcal{S}} | l \rangle = \begin{cases} 0, & k = l = 0, \\ \langle 0 | \hat{Y} | l \rangle, & k = 0, l > 0, \\ \langle k | \hat{Y}^\dagger | 0 \rangle, & k > 0, l = 0, \\ \text{undefined}, & k > 0, l > 0, \end{cases} \quad (\text{A11})$$

The form of  $\hat{Y}$  that satisfies Eq. (A11) for all  $k > 0, l > 0$  is the following:

$$\hat{\mathcal{S}}^\dagger \hat{\mathcal{D}}^\dagger \hat{Y} \hat{\mathcal{D}} \hat{\mathcal{S}} = \hat{Y} + \hat{Y}^\dagger + \hat{a}^\dagger \hat{Q} \hat{a} = -2\hat{p} \circ (\sqrt{2}\alpha e^r + \hat{x} \sinh 2r) + \hat{a}^\dagger \hat{Q} \hat{a}, \quad (\text{A12})$$

where  $\hat{Q}$  is an arbitrary Hermitian operator.

The last term in Eq. (A12) arises due to the non-uniqueness of the operator  $\hat{Y}$ , briefly discussed in Ref. [29]. The choice of  $\hat{Q}$  does not affect the best sensitivity value  $\Delta\phi_0$ , defined by the QCRB (10), but could affect the values of  $\Delta\phi$  for  $\phi \neq 0$ . In this paper, we consider the case of  $\hat{Q} = 0$ , which corresponds to simplest bilinear form of  $\hat{Y}$ .

Rolling back the squeeze and displacement operators, we obtain Eq. (36).

## Appendix B: Threshold detection, two-arm interferometer case

In the two-arm interferometer case, Eqs. (A1) and (A3) take the following form:

$$\hat{\rho}(\phi) = \hat{\mathcal{R}}_-(\phi) \hat{\rho}_{0,0} \hat{\mathcal{R}}_-(\phi), \quad (\text{B1})$$

$$i[\hat{\rho}_{0,0} \hat{N}_-] = \hat{\rho}_{0,0} \circ \hat{Y}, \quad (\text{B2})$$

where

$$\hat{\rho}_{0,0} = |\psi_{0,0}\rangle\langle\psi_{0,0}| \quad (\text{B3})$$

Let the states  $|\psi_{k_1, k_2}\rangle$ , where  $k_{1,2} = 1, 2, \dots$ , complement  $|\psi_{0,0}\rangle$  to the two-dimensional full orthonormal set:

$$\langle\psi_{k_1, k_2}|\psi_{l_1, l_2}\rangle = \delta_{k_1, l_1} \delta_{k_2, l_2}, \quad \sum_{k_1, k_2=0}^{\infty} |\psi_{k_1, k_2}\rangle\langle\psi_{k_1, k_2}| = \hat{I}. \quad (\text{B4})$$

Using this representation, Eq. (B2) can be solved explicitly:

$$\langle\psi_{k_1, k_2}|\hat{Y}|\psi_{l_1, l_2}\rangle = \begin{cases} 0, & k_1 = k_2 = l_1 = l_2 = 0, \\ 2i\langle\psi_{0,0}|\hat{N}_-|\psi_{l_1, l_2}\rangle, & k_1 = k_2 = 0, l_1 + l_2 > 0, \\ -2i\langle\psi_{k_1, k_2}|\hat{N}_-|\psi_{0,0}\rangle, & k_1 + k_2 > 0, l_1 = l_2 = 0, \\ \text{undefined,} & k_1 + k_2 > 0, l_1 + l_2 > 0. \end{cases} \quad (\text{B5})$$

It follows from this solution that

$$(\Delta Y)^2 = 4(\Delta N_-)^2. \quad (\text{B6})$$

As a result, we obtain Eq. (61).

Let us construct now a possible explicit form of  $\hat{Y}$ . The two-dimensional analog of the states (A8) is the following:

$$|\psi_{n_1, n_2}\rangle = \hat{\mathcal{V}}|n_1, n_2\rangle, \quad n_{1,2} = 0, 1, \dots, \quad (\text{B7})$$

where

$$\hat{\mathcal{V}} = \hat{\mathcal{D}}_1 \hat{S}_1 \hat{S}_2, \quad (\text{B8})$$

the operators  $\hat{\mathcal{D}}_1, \hat{S}_{1,2}$  are given by Eqs. (43) and (44), and  $|n_1, n_2\rangle$  are the two-dimensional Fock states. Correspondingly, Eq. (B5) gives:

$$\langle k_1, k_2|\hat{\mathcal{V}}^\dagger \hat{Y} \hat{\mathcal{V}}|l_1, l_2\rangle = \begin{cases} 0, & k_1 = k_2 = l_1 = l_2 = 0, \\ \langle 0, 0|\hat{\mathcal{Y}}_2|l_1, l_2\rangle, & k_1 = k_2 = 0, l_1 + l_2 > 0, \\ \langle k_1, k_2|\hat{\mathcal{Y}}_2^\dagger|0, 0\rangle, & k_1 + k_2 > 0, l_1 = l_2 = 0, \\ \text{undefined,} & k_1 + k_2 > 0, l_1 + l_2 > 0, \end{cases} \quad (\text{B9})$$

where

$$\hat{\mathcal{Y}}_2 = 2i(\alpha\hat{a}_2 e^r + \hat{a}_1 \hat{a}_2 \sinh R_+), \quad (\text{B10})$$

$$R_+ = R + r. \quad (\text{B11})$$

We define  $\hat{Y}$  for all  $k_{1,2} > 0, l_{1,2} > 0$  as follows:

$$\hat{\mathcal{V}}^\dagger \hat{Y} \hat{\mathcal{V}} = \hat{\mathcal{Y}}_2 + \hat{\mathcal{Y}}_2^\dagger = -2[\sqrt{2}\alpha\hat{p}_2 e^r + (\hat{x}_1 \hat{p}_2 + \hat{x}_2 \hat{p}_1) \sinh R_+] \quad (\text{B12})$$

(we omit for brevity the additional operator  $Q$ , see discussion after Eq. (A12)).

Therefore,

$$\hat{Y} = \hat{\mathcal{V}}(\hat{\mathcal{Y}}_2 + \hat{\mathcal{Y}}_2^\dagger)\hat{\mathcal{V}}^\dagger \quad (\text{B13})$$

which gives Eqs. (66) and (67).

Let now  $R = 0$  and  $|\phi| \ll 1$ . In this case, the cumbersome but straightforward calculations give that

$$G = \frac{\partial \langle \hat{Y}_{\text{out}} \rangle}{\partial \phi} = 4(\alpha^2 e^{2r} + \sinh^2 r), \quad (\text{B14a})$$

$$(\Delta \hat{Y}_{\text{out}})^2 = 4\{\alpha^2 e^{2r} + \sinh^2 r + [\alpha^2 e^{2r}(\cosh r + 2 \sinh r)^2 + 4 \cosh^2 r \sinh^2 r]\phi^2\}. \quad (\text{B14b})$$

---

[1] R. Demkowicz-Dobrzanski, M. Jarzyna, and J. Kolodynski, Chapter four - quantum limits in optical interferometry, *Progress in Optics* **60**, 345 (2015).

[2] U. L. Andersen, O. Glöckl, T. Gehring, and G. Leuchs, Quantum interferometry with gaussian states, in *Quantum Information* (John Wiley & Sons, Ltd, 2019) Chap. 35, pp. 777–798, <https://onlinelibrary.wiley.com/doi/10.1002/9783527805785.ch35>.

[3] D. Salykina and F. Khalili, Sensitivity of quantum-enhanced interferometers, *Symmetry* **15**, 774 (2023).

[4] C. M. Caves, Quantum-mechanical noise in an interferometer, *Phys. Rev. D* **23**, 1693 (1981).

[5] <https://www.ligo.org>.

[6] <http://www.virgo-gw.eu>.

[7] Wenxuan Jia et all, Squeezing the quantum noise of a gravitational-wave detector below the standard quantum limit, *Science* **385**, 1318 (2024), <https://www.science.org/doi/pdf/10.1126/science.ado8069>.

[8] R. S. Bondurant and J. H. Shapiro, Squeezed states in phase-sensing interferometers, *Phys. Rev. D* **30**, 2548 (1984).

[9] M. J. Holland and K. Burnett, Interferometric detection of optical phase shifts at the heisenberg limit, *Phys. Rev. Lett.* **71**, 1355 (1993).

[10] J. Bollinger, W. M. Itano, D. J. Wineland, and D. J. Heinzen, Optimal frequency measurements with maximally correlated states, *Phys. Rev. A* **54**, R4649 (1996).

[11] R. Demkowicz-Dobrzański, J. Kołodyński, and M. Guță, The elusive heisenberg limit in quantum-enhanced metrology, *Nature Communications* **3**, 1063 (2012).

[12] L. Pezzè, P. Hyllus, and A. Smerzi, Phase-sensitivity bounds for two-mode interferometers, *Phys. Rev. A* **91**, 032103 (2015).

[13] W. H. Zurek, Decoherence, einselection, and the quantum origins of the classical, *Rev. Mod. Phys.* **75**, 715 (2003).

[14] M. Barbieri, Optical quantum metrology, *PRX Quantum* **3**, 010202 (2022).

[15] W. Górecki, Heisenberg limit beyond quantum fisher information (2023), [arXiv:2304.14370 \[quant-ph\]](https://arxiv.org/abs/2304.14370).

[16] G. Summy and D. Pegg, Phase optimized quantum states of light, *Optics Communications* **77**, 75 (1990).

[17] A. Bandilla, H. Paul, and H. H. Ritze, Realistic quantum states of light with minimum phase uncertainty, *Quantum Optics: Journal of the European Optical Society Part B* **3**, 267 (1991).

[18] M. J. Hall, Phase resolution and coherent phase states, *Journal of Modern Optics* **40**, 809 (1993), <https://doi.org/10.1080/09500349314550841>.

[19] M. J. W. Hall, D. W. Berry, M. Zwierz, and H. M. Wiseman, Universality of the heisenberg limit for estimates of random phase shifts, *Phys. Rev. A* **85**, 041802 (2012).

- [20] M. J. W. Hall and H. M. Wiseman, Heisenberg-style bounds for arbitrary estimates of shift parameters including prior information, *New Journal of Physics* **14**, 033040 (2012).
- [21] W. Górecki, R. Demkowicz-Dobrzański, H. M. Wiseman, and D. W. Berry,  $\pi$ -corrected heisenberg limit, *Phys. Rev. Lett.* **124**, 030501 (2020).
- [22] S. L. Danilishin and F. Y. Khalili, Quantum measurement theory in gravitational-wave detectors, *Living Reviews in Relativity* **15**, 5 (2012).
- [23] J. Aasi *et al*, Advanced ligo, *Classical and Quantum Gravity* **32**, 074001 (2015).
- [24] L. Pezzé and A. Smerzi, Mach-zehnder interferometry at the heisenberg limit with coherent and squeezed-vacuum light, *Phys. Rev. Lett.* **100**, 073601 (2008).
- [25] C. Sparaciari, S. Olivares, and M. G. A. Paris, Gaussian-state interferometry with passive and active elements, *Phys. Rev. A* **93**, 023810 (2016).
- [26] S. Ataman, A. Preda, and R. Ionicioiu, Phase sensitivity of a mach-zehnder interferometer with single-intensity and difference-intensity detection, *Phys. Rev. A* **98**, 043856 (2018).
- [27] C. W. Helstrom, Detection theory and quantum mechanics, *Information and Control* **10**, 254 (1967).
- [28] C. W. Helstrom, Quantum detection and estimation theory (Academic Press, New York, 1976) p. 309.
- [29] C. Oh, C. Lee, C. Rockstuhl, H. Jeong, J. Kim, H. Nha, and S.-Y. Lee, Optimal gaussian measurements for phase estimation in single-mode gaussian metrology, *npj Quantum Information* **5**, 10 (2019).
- [30] R. Yanagimoto, E. Ng, M. Jankowski, R. Nehra, T. P. McKenna, T. Onodera, L. G. Wright, R. Hamerly, A. Marandi, M. M. Fejer, and H. Mabuchi, Mesoscopic ultrafast nonlinear optics&#x2014;the emergence of multimode quantum non-gaussian physics, *Optica* **11**, 896 (2024).
- [31] Y. Gao and H. Lee, Bounds on quantum multiple-parameter estimation with gaussian state, *The European Physical Journal D* **68**, 347 (2014).
- [32] R. Nichols, P. Liuzzo-Scorpo, P. A. Knott, and G. Adesso, Multiparameter gaussian quantum metrology, *Phys. Rev. A* **98**, 012114 (2018).
- [33] M. D. Lang and C. M. Caves, Optimal quantum-enhanced interferometry using a laser power source, *Phys. Rev. Lett.* **111**, 173601 (2013).
- [34] H. F. Hofmann, All path-symmetric pure states achieve their maximal phase sensitivity in conventional two-path interferometry, *Phys. Rev. A* **79**, 033822 (2009).
- [35] M. Manceau, F. Khalili, and M. Chekhova, Improving the phase super-sensitivity of squeezing-assisted interferometers by squeeze factor unbalancing, *New Journal of Physics* **19**, 013014 (2017).